Proceedings of the ASME 2021
International Mechanical Engineering Congress and Exposition
IMECE2021
November 1-5, 2021, Virtual Conference, Online

IMECE2021-70054

ENHANCED POOL BOILING CRITICAL HEAT FLUX ON TILTED HEATING SURFACES USING COLUMNAR-POST WICKS

Mohammad Borumand and Gisuk Hwang

Department of Mechanical Engineering, Wichita State University, Wichita, KS, 67260

ABSTRACT

The upper heat flux limit of nucleate pool-boiling heat transfer (NPHT), i.e., Critical Heat Flux (CHF), results in system burnouts in various energy and industrial applications, and the understandings of the tailored CHF mechanisms are crucial to develop robust thermal management systems. In various applications, the understandings of the tailored CHF mechanisms are essential for design flexibility and operation sustainability, but previous CHF tailoring studies focused on upward-facing heater orientation. This study examines the tailored hydrodynamic-instability using columnar post wick array to enhance CHF on tilted heater surfaces (with surface orientation θ = 60°-130°). Liquid supply enhances via the capillary flow through the post wicks, while the produced vapor efficiently escapes through pore space among the post wicks. The enhanced CHF are predicted using a modified interfacial lift-off CHF hydrodynamic model that relies on classical two-dimensional interfacial instability theory. On the tilted plain surface with the surface orientation from 60° to 130°, the model predicts the CHF, q_{CHF} = 126.5 to 92.5 W/cm^2 at the critical hydrodynamic instability wavelength, λ_{cr} = 9.2 to 12.7 mm, respectively, using water as a working fluid. The enhanced CHF is predicted at the surface orientations of θ = 90° and 120°, showing a maximum of 185% and 250% increase, respectively. The maximum enhancement occurs at the smallest columnar-post pitch distances, l_p = 2.5 mm, where q_{CHF} increases from 104 to 295 W/cm^2 for θ = 90°, and from 89 to 313 W/cm^2 for θ = 120°. The developed model will provide insights into the tailored hydrodynamic instability wavelength at tilted angle via engineered surface.

Keywords: hydrodynamic-instability wavelength, chocking limit, capillary flow, interfacial lift-off model, liquid-vapor phase separation

NOMENCLATURE

A_l	upstream wetting front area, m^2
A_{cp}	engineered upstream wetting front area, m^2
A_p	unit plain surface area, m^2
b	ratio of wetting front length to vapor wavelength on the plain surface, l/λ
b_1	ratio of base diameter of columnar-post to intercolumnar spacing, d_{cp} / l_p
b_2	ratio of wetting front area to unit plain surface area, A_{cp} / A_p
c_p	specific heat of liquid at constant pressure, J/K.kg
d_{cp}	columnar-post wick diameter, m
g_e	Earth's gravity, m/s^2
H	mean layer thickness, m
Δh_{fg}	latent heat of vaporization, J/kg
k_{cr}	critical wave number
l	wetting front length on plain surface, m
l_p	intercolumnar spacing, m
L	heater length, m
p	pressure, Pa
$\overline{p_f - p_g}$	average interfacial pressure difference at wetting front, Pa
q	heat flux, W/m^2
q_{CHF}	Critical Heat Flux (CHF), W/m^2
q_l	heat flux concentrated at a wetting front, W/m^2
u_g	mean velocity of vapor phase, m/s
W	heater width, m
z	streamwise coordinate, m
z^*	distance from leading edge of heater to center of first wetting front [$z^* = \lambda_{cr}$]

Greek symbols

θ	surface orientation angle measured from horizontal upward-facing position, °
ΔT_{sub}	subcooled temperature, K
δ	mean vapor layer thickness, m
λ	vapor wavelength, m
λ_{cr}	critical wavelength, m
$\lambda_{cr,cp}$	controlled critical wavelength using columnar-post wick, m
μ	dynamic viscosity, Pa-s
ρ	density, kg/m^3

ρ'' modified density, kg/m^3
σ surface tension, N/m
τ_i interfacial shear stress, Pa

Subscript
f saturated liquid
g saturated vapor
p plain surface

1. INTRODUCTION

To meet the demands of miniaturization and increased system power, two-phase high heat flux thermal management systems are growing at a rapid pace [1]. A nucleate pool boiling system is a typical two-phase thermal control system that offers high cooling capacity through the phase-change of a working fluid, however, the maximum cooling capacity is limited by the upper heat transfer limit, known as Critical Heat Flux (CHF). At CHF, the liquid supply is chocked by excessive vapor generation near the heating surface, and this causes premature surface dry-out and subsequent operation failure. Extensive research has shown that among the numerous interlinked design/operation parameters such as heater size, shape, surface wetting, working fluid properties, and system pressure that could potentially lead to premature occurrence of CHF, the key contributor is the hydrodynamic-instability of the liquid-vapor interface [2,3].

It has been shown that among the different CHF controlling mechanisms such as the kinetic evaporation limit, the viscous drag liquid limit, and hydrodynamic instability liquid-chocking limit, CHF is dominated by the hydrodynamic instability liquid-chocking limit [4]. Numerous studies have shown that the critical instability wavelength can be tailored using engineered surface at the horizontal heater surface, i.e., upward facing heater surface. Liter and Kaviany showed that pool boiling CHF can be enhanced up to three times over that of a plain surface using modulated porous-layer coatings, i.e., wicks [4]. It has been concluded that wick non-uniformity separates the liquid and vapor phases, thus reducing the liquid vapor counterflow resistance adjacent to the surface [4,5]. These studies are primarily focused on horizontal heater surfaces, i.e., upward-facing heater surfaces. However, the in-depth study of the tailored CHF on the tilted heater surface is rare, although the understandings of enhanced CHF on such surface orientations are crucial to delay the catastrophic surface dryout for flexible system design and safe operation.

Howard and Mudawar [6] studied pool boiling on heating surfaces with near-vertical orientations with respect to upward facing surface, i.e. θ = 60°-130°, and developed a mathematical model for prediction of CHF in which the lift-off of the liquid-vapor interface was considered as the CHF triggering mechanism. Their model utilizes continuity, momentum and energy balances along with hydrodynamic instability theory to accounts for the hydrodynamic instability wavelength and "wetting front" length. However, the potential of pool boiling tailored "wetting front" using wick structures have not been thoroughly investigated.

In this study, pool boiling CHF enhancement on tilted surfaces through tailored hydrodynamic-instability wavelength has been studied. In section 2, the physical model is presented followed by a mathematical formulation of CHF on plain surfaces and post-columnar wick structures in Section 3. In section 4, the predicted CHF enhancement using columnar-post wicks has been presented for two different heating surface orientations and a discussion is provided. Finally, a conclusion will be made.

2. Physical Model

Photographic and high-speed video-imaging studies shows that excessive vapor generation at near-CHF on tilted (near-vertical) surface orientations, i.e., 60°-150°, produce a series of clusters of wave-like vapor patches that sweep along the heating surface. Figure 1 depicts the idealized (sinusoidal) wavy liquid-vapor interface with minimum liquid contact points with the plain heated surface, so called, wetting fronts.

3. Mathematical Model for Pool Boiling CHF

In this section, the original interfacial lift-off model, which incorporates four major sub-models, is briefly introduced followed by a detailed explanation of the modified interfacial lift-off model. The detailed model descriptions are found in the previous work [6]

The interfacial lift-off model predicts the mean velocity of vapor phase, u_g, through a one-dimensional separated flow model by applying conservation of mass and energy to a vapor control-volume of length dz, where z is the buoyancy-driven flow direction. Integrating the differential mass and energy equations over the z yields Eq. (1)

$$\rho_g u_g \delta = \frac{qz}{\Delta h_{fg}[1+\frac{c_P \Delta T_{sub}}{\Delta h_{fg}}]} \tag{1}$$

where q is the heat flux, z is the streamwise coordinate, u_g is the vapor mean velocity, ρ_g is the vapor density, δ is the vapor layer thickness, c_p is the liquid specific heat at constant pressure, ΔT_{sub} is the subcooled temperature, and Δh_{fg} is the latent heat of vaporization.

Applying a momentum balance on the same vapor control volume without inclusion of the negligible wall interfacial shear stress results in Eq. (2)

$$\frac{\mathrm{d}}{\mathrm{d}z}[\rho_g u_g^2 \delta] = \delta(\rho_f - \rho_g) g_e \sin\theta - \tau_i \tag{2}$$

where θ is the orientation angle measured from the horizontal upward-facing position and $\tau_i = 0.5 f \rho u_g^2$ is the interfacial shear stress with friction factor $f_i = 0.5$ [6]. Combining Eqs. (1) and (2) results in the following differential equation relating u_g to z

$$\frac{\mathrm{d}}{\mathrm{d}z}[u_g z] = \frac{(\rho_f - \rho_g) g_e \sin\theta}{\rho_g} \frac{z}{u_g} - \frac{\tau_i \Delta h_{fg}[1+\frac{c_P \Delta T_{sub}}{\Delta h_{fg}}]}{q} \tag{3}$$

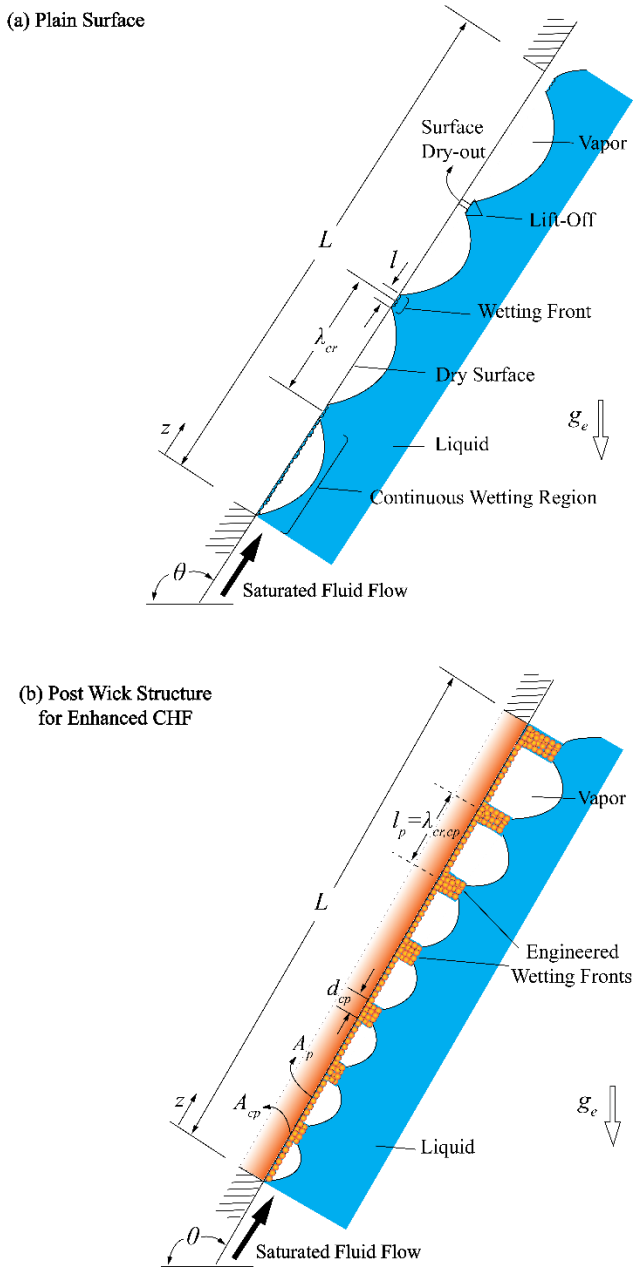

Figure 1. Schematic of the pool boiling wavy vapor layer on tilted heating surface at Critical Heat Flux (CHF) on (a) the plain surface, and (b) the columnar-post wick.

which is solved numerically using the Euler method.

The vapor mean velocity is then incorporated into a classical hydrodynamic instability analysis to determine the critical wavelength, λ_{cr}, assuming irrotational, inviscid and incompressible flow with a sinusoidal liquid-vapor interface with small curvature.

$$k_{cr} = \frac{2\pi}{\lambda_{cr}} = \frac{\rho_f'' \rho_g'' (u_g)^2}{2\sigma(\rho_f'' + \rho_g'')} + \sqrt{\left[\frac{\rho_f'' \rho_g'' (u_g)^2}{2\sigma(\rho_f'' + \rho_g'')}\right]^2 + \frac{(\rho_f - \rho_g) g_e \cos\theta}{\sigma}} \quad (4)$$

In Eq. (4), the k_{cr} is the critical wave number, λ_{cr} is the critical wavelength, σ is the surface tension, g_e is the Earth's gravity, and the modified density terms for liquid and vapor are given by $\rho''_f = \rho_f \coth(k_{cr}H_f)$ and $\rho''_g = \rho_g \coth(k_{cr}H_g)$, respectively. To obtain λ_{cr}, the Eq. (4) should be solved iteratively since λ_{cr} is contained in the modified density terms ρ''_f and ρ''_g.

The third sub-model constitutes an instantaneous energy balance that relates the average heat flux over the entire heated surface to the localized heat fluxes concentrated in all the wetting fronts. The final element of interfacial lift-off model is the lift-off criterion which postulates the lifting-off of the most upstream wetting front as the trigger mechanism for CHF, and this occurs when the normal momentum flux of the vapor generated at the wetting front just exceeds the pressure force that maintains the interfacial contact. This is given as

$$q_l = \rho_g \Delta h_{fg} \left(1 + \frac{c_p \Delta T_{sub}}{\Delta h_{fg}}\right)\left[\frac{\overline{p_f - p_g}}{\rho_g}\right]^{1/2} \quad (5)$$

where q_l is the localized heat flux at a wetting front, and $\overline{p_f - p_g}$ is the average interfacial pressure difference at the upstream wetting front. The Eq. (5) yields the desired expression for the local lift-off heat flux. Therefore, the local heat flux associated with interfacial lift-off can be found.

The next section describes analytical expressions to find the average pressure difference and to relate the local lift-off heat flux q_l to the critical heat flux q_{CHF}. These differ between the plain surface and columnar-post wick structure, due to the different dimension of the vapor wavelengths and wetting front associated with each case.

A) Plain Surface

For a plain surface, the average interfacial pressure difference can be found by integrating the product of surface tension and interfacial curvature over the wetting fronts (see Figure 1). This leads to Eq. (6)

$$\overline{p_f - p_g} = 8\sqrt{2}\pi b \frac{\sigma\delta}{\lambda_{cr}^2} \quad (6)$$

where $b = l/\lambda$ is the ratio of the wetting front length to the vapor wavelength. The extensive flow visualization studies on pool boiling on near-vertical surface has shown that b = 0.25 for nearly-saturated FC-72 working fluid [6].

Assuming that heat transfer occurs only at the wetting fronts and that heater surface regions beneath a wave are adiabatic, the CHF can be calculated using Eq. (7),

$$q_{\mathrm{CHF}} = b q_l(z^*). \quad (7)$$

Based on Eq. (7), the ratio of CHF to wetting front lift-off heat flux is the same as the ratio of wetting front length to vapor wave wavelength.

B) Columnar-Post Wick Structure

The average interfacial pressure difference and b are completely different for a heating surface with columnar-post wick structure. Here, the engineered wetting front's length is approximated as the diameter of the columnar-post wick, d_{cp}, and

the tailored critical vapor wavelength on columnar-post wick is shown by $\lambda_{cr,cp}$. Integrating the pressure difference over the engineered wetting front leads to Eq. (8)

$$\overline{p_f - p_g} = \frac{-\pi\sigma\delta}{\lambda_{cr}}[\sin(\pi(1+b_1)) - \sin(\pi(1-b_1))] \quad (8)$$

where $b_1 = d_{cp}/\lambda_{cr,cp}$ is the ratio of the columnar-post wick diameter to tailored critical wavelength.

The width of the wetting front is the second difference between the plain surface and columnar-post wick. Contrary to the plain surface where the wetting front touches the entire width of the heater, the tailored wetting front of the columnar-post wick touches only a portion of the columnar-post wick diameter due to the capillary flow through the wicks. Following the main postulate that heat transfer occurs only beneath the tailored wetting front and that the region beneath vapor waves are essentially adiabatic, b in Eq. (7) should be changed to $b_2 = A_{cp}/A_p$. This states that the ratio of CHF to lift-off heat flux is equal to the ratio of engineered wetting front area to unit plain surface area.

$$q_{\mathrm{CHF}} = b_2 q_l(z^*) \quad (9)$$

which yields the tailored CHF on a tilted heater with columnar-post wick structure.

Due to the coupling of the four sub-models, i.e., Eq. (1) to (9), it uses an iterative numerical method.

4. RESULTS AND DISCUSSION

In this section, the interfacial lift-off model is first validated by comparing pool boiling CHF and λ_{cr} results on tilted plain surface with available experimental and numerical data for FC-72 working fluid. CH and λ_{cr} would also be predicted for water as the most widely available working and CHF predictions are compared with available predictions and experimental results [2–4,6–8]. Finally, CHF enhancement on post-columnar wick structures with water working fluid would be discussed for two different surface orientations.

A) CHF on Tilted Plain Surface

Figure 2 shows the predicted critical hydrodynamic instability wavelength, λ_{cr}, using Eq. (4) as a function of heater orientation for FC-72 over a range of heater surface orientations, $0^o < \theta < 140^o$. The predictions agree with those of Howard and Mudawar [6]. Also, the critical hydrodynamic instability wavelength, λ_{cr} for upward facing heater ($\theta = 0°$) using Zuber theory [2] is also shown. In fact, the predicted critical hydrodynamic instability wavelength using Zuber correlation overpredicts those using Eq. (4) due to assumed bubble departure diameter at CHF. It can be seen from Figure 2 that minimum λ_{cr} occurs at around $\theta = 75°$, since at this heater surface orientation vapor can escape from the heating surface area much more easily than lower heating surface orientations, i.e., $\theta \sim 0°$, or high heating surface orientations, i.e., $\theta \sim 140°$.

Figure 3 shows CHF predictions as a function of surface orientation for FC-72. The results are also compared with the

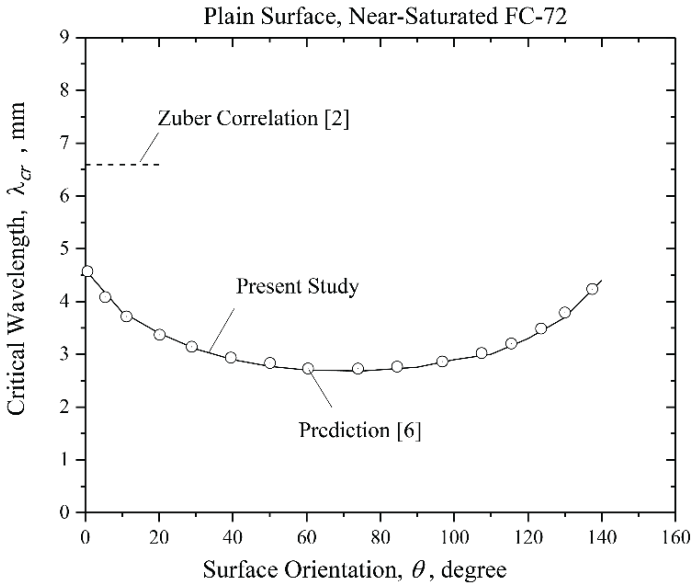

Figure 2: Critical wavelength with respect to the surface orientation for near-saturated FC-72. Previous predictions [6] along with prediction using the Zuber correlation [2] are also shown.

previous experimental and numerical results [1]. The interfacial lift-off CHF model should only be used for $60° \le \theta \le 140°$ where the sweeping wavy liquid-vapor flow regime is present [6]. Figure 3 also shows that CHF decreases with increasing surface orientation until it reaches $\theta \sim 140°$ where the wavy vapor flow regime changes to repeatedly stratified vapor regime associated with downward- facing orientations, i.e., $140° \le \theta \le 180°$. At these surface orientations, vapor scape due to the buoyancy force

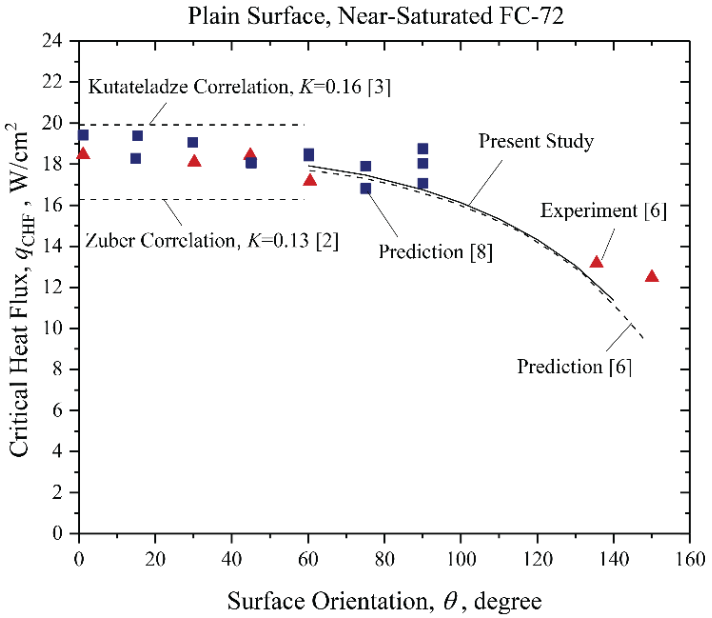

Figure 3: Critical Heat Flux (CHF) with respect to the surface orientation for near-saturated FC-72. Previous experiments and predictions are also shown [2–4,6–8].

is blocked by the heating surface.

Figure 4 shows the predicted critical hydrodynamic instability wavelength, λ_{cr}, as a function of heater orientation for near-saturated water. The relatively large critical hydrodynamic instability wavelength for water, i.e., 9 mm < λ_{cr} < 12.5 mm shows that the CHF can be further tailored by reducing the hydrodynamic instability wavelength using columnar-post wick structures.

Figure 5 shows CHF predictions as a function of surface orientation for water. The results are also compared with the experimental and numerical CHF results [2,3,6,7]. Note that the original interfacial lift-off model is developed and validated for FC-72, but in this study, water is used for larger CHF enhancement via available manufacturing approach. This is achieved by changing the thermophysical properties and using the empirical parameter b = 0.23 and b = 0.25. The curve-fitted b can be validated in future flow visualization study as similarly done in the previous work [6].

A) Tailored CHF on Columnar-Post Wick Structure

Figure 6 shows the predicted CHF enhancement on an upward-facing surface with respect to the hydrodynamic instability wavelength λ_{cr}, using the columnar-post wick [4,9]. As previously discussed, incorporation of columnar-post wick reduces the hydrodynamic instability wavelength and increases surface ratio of the wetting front by effectively changing the vapor generation sites and liquid supply channels as shown in Figure 1.

Figure 7 shows the predicted CHF enhancement with respect to the hydrodynamic instability wavelength λ_{cr}, using the columnar-post wick for vertically-oriented heating surface, θ = 90°. Note that λ_{cr} = 9.3 mm on the plain surface based on Figure 4, and as the inter-columnar spacing, l_p, reduces to 2.5 mm

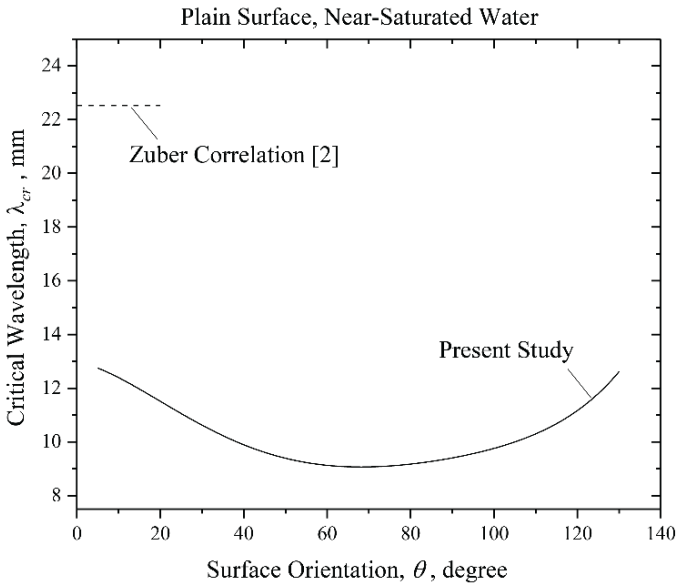

Figure 4: Critical wavelength λ_{cr}, with respect to the surface orientation for near-saturated water. Prediction using the Zuber correlation is also shown [2].

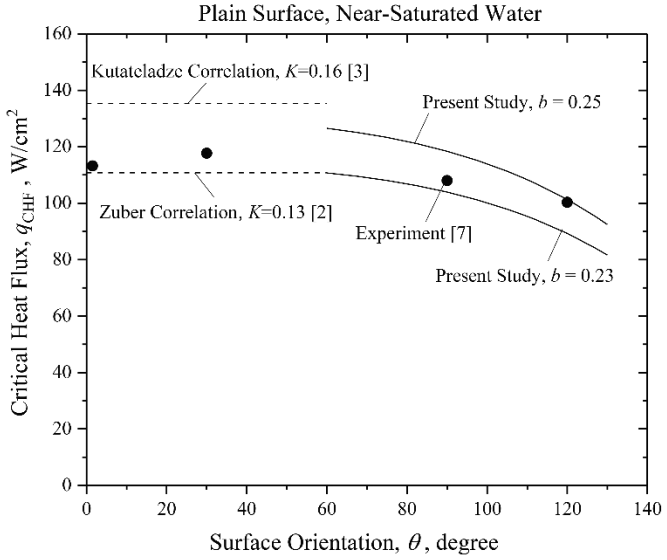

Figure 5: Critical Heat Flux (CHF) with respect to the surface orientation for near-saturated water. Previous experiments and predictions are also been shown [2,3,7].

(manufacturing limit), the CHF exponentially increases by decreasing the critical hydrodynamic instability wavelength and increasing the relative wetting front surface area, b_1 and b_2 in Eqs. (8) and (9). The maximum enhanced CHF is predicted as q_{CHF} = 300 W/cm^2 (nearly 1.85 times higher than that of the plain surface, q_{CHF} = 102.5 W/cm^2), and this is limited by the manufacturing limit. In fact, the predicted CHF at λ_{cr} = 9.3 mm is smaller than the experimental result on the plain surface, q_{CHF} = 152.5 W/cm^2, and this reduced CHF is related to the reduced b_2 in Eq. (9), i.e., reduced relative wetting front areas by the

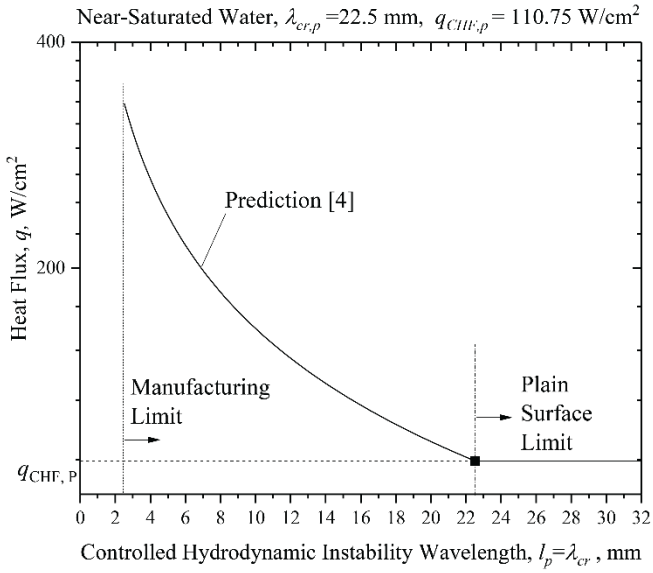

Figure 6: CHF enhancement as a function of controlled critical wavelength, λ_m, using post-columnar wick with water as working fluid. The plain surface critical wavelength, $\lambda_{cr,p}$, and critical heat flux, $q_{CHF,p}$, are also shown [4,9].

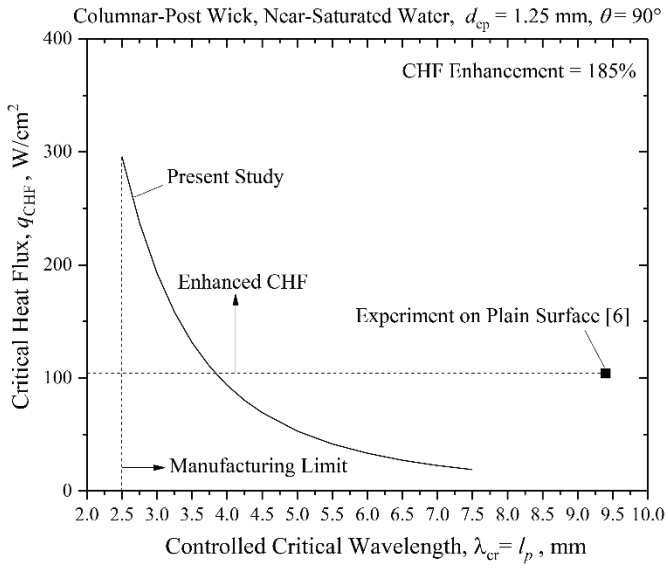

Figure 7: Enhanced Critical Heat Flux (CHF) with respect to the controlled hydrodynamic instability wavelength using the columnar-post wick along with varying b_1 and b_2 (θ = 90°) [6].

columnar-posts i.e., the columnar-post wicks allow for tailored wetting front by forming it at the tips of columnar-post wicks. At CHF, heat transfer occurs only over the wetting front area, and since for high l_p the overall heat transfer area decreases, the heat transfer also decreases. Note that the CHF is also related to the effective vapor layer thickness [see Eq. (8)], however, for the simple treatment, the predicted δ on the plain surface is used assuming that the columnar-post wick height is manufactured as the same height as the predicted δ. Further study is necessary to determine the modified δ due to the columnar-post wick.

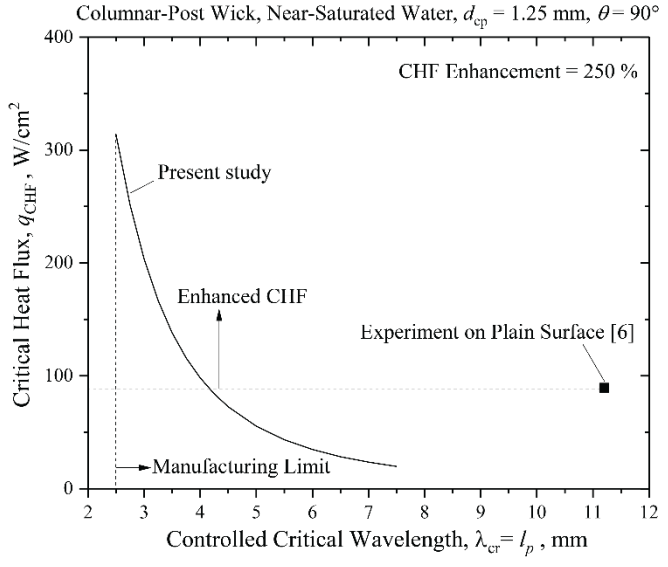

Figure 8: Enhanced Critical Heat Flux (CHF) with respect to the controlled hydrodynamic instability wavelength using the columnar-post wick along with varying b_1 and b_2 (θ = 120°) [6].

Figure 8 shows the predicted CHF enhancement with respect to the hydrodynamic instability wavelength λ_{cr}, using the columnar-post wick for θ = 120°, postulating tailoring hydrodynamic instability wavelength via post wicks. The same principles apply. However, due to the higher hydrodynamic instability wavelength (λ_{cr} =11.4 mm), more CHF improvement is expected using the columnar-post wick structure. Figure 11 shows that the CHF is nearly 2.5 times higher than that of the plain surface for θ = 120°.

5. CONCLUSION

In this study, the original interfacial lift-off model is modified to investigate enhanced pool boiling Critical Heat Flux (CHF) on tilted heating surfaces through tailored hydrodynamic-instability wavelength using columnar-post wicks. The CHF model is first validated by comparing CHF and critical hydrodynamic instability wavelength predictions, λ_{cr}, with available predictions and experiments on plain surface over a range of heating surface orientations, θ = 60° - 130° using FC-72 and water. The model is then modified by adjusting the empirical coefficient, b, to account for tailored λ_{cr}, and to explore the potential CHF enhancement for two different heating surface orientations, θ = 90° and 120°, using water due to its large critical hydrodynamic instability wavelength, $\lambda_{cr} \sim$ 7.5 mm. It is shown that the CHF enhances for small post wick pitch distances, l_p < 4 mm with a maximum up to 2.5 times compared to plain surface at θ = 120° and l_p = 2.5 mm. However, this work does not consider the expected fluid flow and vapor layer thickness changes due to the presence of the post wicks, and these will be further study.

ACKNOWLEDGEMENTS

The authors are thankful for financial support by the National Science Foundation (NSF), Award No. OIA-1929187, and the Wichita State University Convergence Sciences Initiative Program. This work is also financially supported by the College of Engineering, Department of Mechanical Engineering, Wichita State University.

REFERENCES

[1] Mudawar, I., 2001, "Assessment of High-Heat-Flux Thermal Management Schemes," IEEE Trans. Compon. Packag. Technol., **24**(2), pp. 122–141.

[2] Zuber, N., 1959, *Hydrodynamic Aspects of Boiling Heat Transfer*, University of California, Los Angeles, CA, University of California, Los Angeles, Ph.D. Thesis.

[3] Kutateladze, S. S. (Samson S. and U.S. Atomic Energy Commission., 1959, *Heat Transfer in Condensation and Boiling*, U.S. Atomic Energy Commission, Technical Information Service, [Washington].

[4] Liter, S. G., and Kaviany, M., 2001, "Pool-Boiling CHF Enhancement by Modulated Porous-Layer Coating: Theory

and Experiment," Int. J. Heat Mass Transf., **44**(22), pp. 4287–4311.
[5] Nasersharifi, Y., Kaviany, M., and Hwang, G., 2018, "Pool-Boiling Enhancement Using Multilevel Modulated Wick," Appl. Therm. Eng., **137**, pp. 268–276.
[6] Howard, A. H., and Mudawar, I., 1999, "Orientation Effects on Pool Boiling Critical Heat Flux (CHF) and Modeling of CHF for near-Vertical Surfaces," Int. J. Heat Mass Transf., **42**(9), pp. 1665–1688.
[7] Yang, S. H., Baek, W.-P., and Chang, S. H., 1997, "Pool-Boiling Critical Heat Flux of Water on Small Plates: Effects of Surface Orientation and Size," Int. Commun. Heat Mass Transf., **24**(8), pp. 1093–1102.
[8] Mudawar, I., Howard, A., and Gersey, C., 1997, "An Analytical Model for Near-Saturated Pool Boiling Critical Heat Flux on Vertical Surfaces," Int. J. Heat Mass Transf., **40**, pp. 2327–2339.
[9] Nasersharifi, Y., Kaviany, M., and Hwang, G., 2018, "Pool-Boiling Enhancement Using Multilevel Modulated Wick," Appl. Therm. Eng., **137**, pp. 268–276.